International Journal of Earth, Energy and Environmental Sciences
ISSN: 2517-942X
Vol:15, No:8, 2021

Thin Bed Reservoir Delineation Using Spectral Decomposition and Instantaneous Seismic Attributes, Pohokura Field, Taranaki Basin, New Zealand

P. Sophon, M. Kruachanta, S. Chaisri, G. Leaungvongpaisan, P. Wongpornchai‡

***Abstract*—**The thick bed hydrocarbon reservoirs are primarily interested because of the more prolific production. When the amount of petroleum in the thick bed starts decreasing, the thin bed reservoirs are the alternative targets to maintain the reserves. The conventional interpretation of seismic data cannot delineate the thin bed having thickness less than the vertical seismic resolution. Therefore, spectral decomposition and instantaneous seismic attributes were used to delineate the thin bed in this study. Short Window Discrete Fourier Transform (SWDFT) spectral decomposition and instantaneous frequency attributes were used to reveal the thin bed reservoir, while Continuous Wavelet Transform (CWT) spectral decomposition and envelope (instantaneous amplitude) attributes were used to indicate hydrocarbon bearing zone. The study area is located in the Pohokura Field, Taranaki Basin, New Zealand. The thin bed target is the uppermost part of Mangahewa Formation, the most productive in the gas-condensate production in the Pohokura Field. According to the time-frequency analysis, SWDFT spectral decomposition can reveal the thin#bed using# 72 Hz SWDFT isofrequency section and map, and that is confirmed by the instantaneous frequency attribute. The envelope attribute showing the high anomaly indicates the hydrocarbon accumulation area at the thin bed target. Moreover, the CWT spectral decomposition shows the low-frequency shadow zone and abnormal seismic attenuation in the higher isofrequencies below the thin bed confirms#that the thin#bed can be a prospective hydrocarbon zone.

***Keywords*—**Hydrocarbon indication, instantaneous seismic attribute, spectral decomposition, thin bed delineation.

I. Introduction

IN petroleum exploration and production, thick-bed hydrocarbon reservoirs are preferable to gain the maximum profit. For the primary stage of production, thick-bed hydrocarbon reservoirs are selected for production. When the amount of petroleum in the thick beds starts decreasing, thin-bed reservoirs could provide opportunities to increase the reserves. A thin-bed reservoir is a bed whose thickness below the seismic tuning thickness; therefore, it cannot be easily delineated by the conventional interpretation of seismic data because of the seismic vertical resolution limitation. In this study, SWDFT and CWT spectral decompositions and instantaneous seismic attributes were selected to reveal the thin beds.

The study area is in the Pohokura Field, Taranaki Basin, New Zealand (Fig. 1). Taranaki Basin is the largest gas and oil region in New Zealand. Pohokura Field is the most productive field in gas-condensate production of the Taranaki Basin. The New Zealand Ministry of Business, Innovation and Employment (NZ MBIE) [1] stated that the remaining reserve of condensate in Pohokura Field at the end of 2016 was 20.2 million barrels. In 2017, OMV (the operating company) produced 2.8 million barrels of condensate. Thus, the remaining condensate reserves should be about 17.4 million barrels at the end of 2017. The revised 2017 condensate reserves were only 13.26 million barrels. This decrease of reserves has significantly affected the remaining NZ national reserves because Pohokura Field is the largest gas-condensate field in the country. This affects the long-run average natural gas prices.

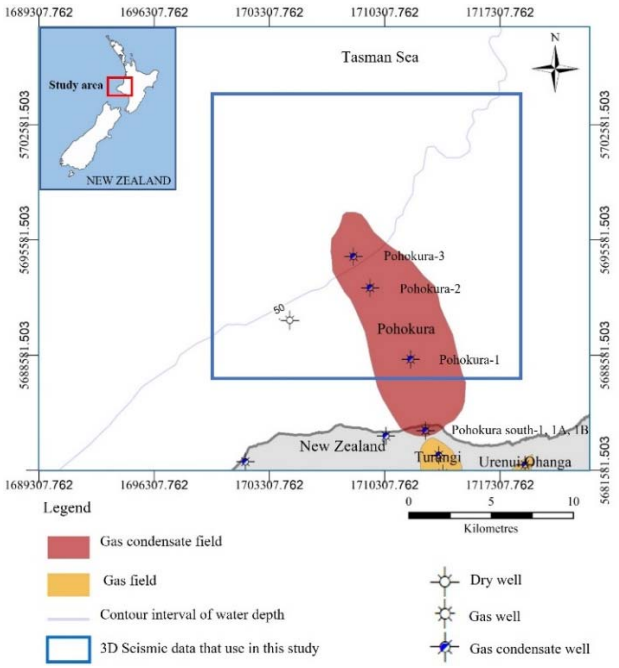

Fig. 1 Location of wells and seismic acquisition area in Pohokura Field used for this study (modified from [2]-[4])

The main reservoir of the Pohokura Field is the Middle to Late Eocene Mangahewa Formation [5]. The depositional environment is paleoshoreline comprising sandstone, coal bed

P. Sophon is with Department of Geological Sciences, Faculty of Science, Chiang Mai University, Chiang Mai, 50200, Thailand (e-mail: phattranit_so@cmu.ac.th).

and sandstone interbedded with fine-grain sedimentary rock. Interfingering of fine- and coarse-grain sediments causes the sandstone in this area to be thin beds [5]. For this reason, the thin bed of the Pohokura Field was mapped in this study.

New Zealand Petroleum and Minerals (NZPM, a branch of MBIE) provided the seismic and well data used in this study. The full-stacked 3D seismic data cover an area of approximately 300 square kilometers with 1,308 inlines and 1,480 crosslines, shown in the blue square in Fig. 1. The seismic data were acquired by Western Geophysical in 1988 using air guns as a seismic source. Available offshore well data, Pohokura-1 and Pohokura-3, were incorporated in the analysis. The well data consist of geophysical wireline logs, deviation surveys, check-shot data, and tops of the formations.

II. Theories and Applications

A. Instantaneous Seismic Attributes

Envelope and instantaneous frequency are the instantaneous seismic attributes which are related to complex seismic traces. The complex seismic trace *z(t)* [6] includes a real component *x(t)* and a quadrature (imaginary) component *y(t)*, which is computed by the Hilbert Transform. The complex trace is defined as [3]#

$$z(t) = x(t) + iy(t) \tag{1}$$

The magnitude of *z(t)* is the envelope *a(t)* attribute (often called "instantaneous amplitude") defined as [6]

$$a(t) = \sqrt{x^2(t) + y^2(t)} \tag{2}$$

A large envelope usually associates with a lithological change between adjacent rock layers, such as a discontinuity or unconformity, or with a hydrocarbon-bearing zone (bright spot), especially a gas accumulation [7]. However, some bright spots are not related to hydrocarbons. Interpreters should be aware of them.

The phase between the real and quadrature components is an instantaneous phase $\theta_i(t)$ attribute. The differential of instantaneous phase is the instantaneous frequency $f_i(t)$ attribute defined as [6]

$$f_i(t) = \frac{1}{2\pi}\frac{d}{dt}\theta_i(t) \tag{3}$$

Spikes of instantaneous frequency largely correspond to the waveform distortion caused by wavelet interference, which can be used to identify the thin beds [6], [8]. Moreover, oil and gas accumulations usually cause a drop-off of high frequency components just below the hydrocarbon reservoir; thus, the local frequency anomaly would be low [9].

B. Spectral Decomposition

Spectral decomposition is the time-frequency analysis to reveal geological features or hydrocarbons that were concealed in the time domain. There are 2 methods of spectral decomposition used in this study, SWDFT and CWT.

SWDFT applies the Fourier Transform at specific times and in overlapping windows, mathematically expressed as [10]

$$SWDFT(\omega,\tau) = \int_{-\infty}^{\infty} f(t)\overline{\emptyset}(t-\tau)e^{-i\omega t}dt \tag{4}$$

where $f(t)$ is the signal, the window function $\emptyset$ is centered at time t = τ, with τ being the translation parameter, $\overline{\emptyset}$ is the complex conjugate of $\emptyset$, and $\overline{\emptyset}(t-\tau)$ is convolved window.

Using spectral decomposition, the reflection from a thin bed has a characteristic expression in the frequency domain that can be used to estimate the temporal bed thickness. For example, the notches in the amplitude spectrum could show the temporal bed thickness of a simple homogeneous thin bed. Usually, however, there is no single and simple bed in the subsurface. Thus, the result is a complicated amplitude spectrum [11]. Therefore, Partyka et al. [11] proposed an approach to visualize the thin bed by using isofrequency maps or sections from SWDFT spectral decomposition. Kwietniak [12] suggested that the optimal window length for SWDFT spectral decomposition should not be too long because the geological features in the interval would be merged and should not be shorter than the thinnest target feature.

CWT is an alternative method in spectral decomposition. CWT spectral decomposition uses the wavelet dilated and translated in seismic signal to get the frequency information defined as [10].

$$F_W(\sigma,\tau) = \int_{-\infty}^{\infty} f(t)\frac{1}{\sqrt{\sigma}}\bar{\psi}\left(\frac{t-\tau}{\sigma}\right)dt \tag{5}$$

where $\bar{\psi}$ is the complex conjugate of ψ, and $F_W(\sigma,\tau)$ is the time-scale map.

There are many wavelet functions such as Morlet, Gaussian, and Mexican Hat. For CWT spectral decomposition in low frequencies, the time resolution is low and the frequency resolution is high, while in high frequencies, the time resolution is high and the frequency resolution is low [10]. Thus, when the time resolution increases, the frequency resolution decreases, and vice versa [13]. Chopra and Marfurt [14] evaluated the relative resultant value of CWT spectral decomposition and usability of the mother wavelets to analyze a fluvial-deltaic system. The Morlet wavelet generated the most robust result. However, the application of the Morlet wavelet could not be generalized due to the nature of the seismic signal acquired in different areas being completely different. Hence results from different mother wavelets should be compared [15].

The CWT spectral decomposition allows delineating the sweet spot reservoir which is related to a low-frequency shadow zone [16]. The sweet spot can be indicated by a high amplitude in the low frequency section (low frequency shadow zone) and the amplitude disappearing in the high-frequency section (abnormal seismic attenuation).

III. Methodologies and Results

The workflow of the study is shown in Fig. 2. Well log analysis, seismic to well correlation, and instantaneous seismic attributes computation were done using Petrel E&P Software

Platform. Spectral decompositions, both SWDFT and CWT, were computed in OpendTect Pro and displayed in Petrel E&P Software Platform for analysis.

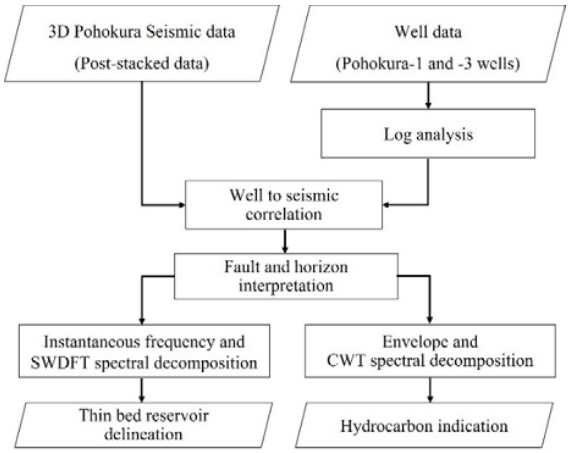

Fig. 2 The workflow of this study.

Top Sandstone Mangahewa (TSM) and bottom Sandstone Mangahewa (BSM) Formations were selected to locate the thin bed reservoir interval. According to the log analysis, the sandstone thickness in Pohokura-1 and 3 wells is about 18 meters. The Top Mangahewa Formation was tied to the seismic data. Synthetic seismograms are generated from the convolution of wavelet and reflectivity. The reflectivity was calculated from the acoustic impedances, which are the multiplication of the density and calibrated velocity logs, which was calibrated by check shot data. The wavelets were extracted from the seismic data around wells using a Petrel deterministic method. The extraction window was about 200 ms long, covering the target zone. The correlation between the synthetic seismogram and seismic data around the well is 0.850 for Pohokura-1 well (Fig. 3) and 0.841 for Pohokura-3 well (Fig. 4). The cross section between Pohokura-1 and Pohukura-3 wells (Fig. 5) shows the well to seismic correlation in seismic data.

Generally, the vertical resolution of the seismic data is one-quarter of the wavelength [17], which is computed using the velocity and dominant frequency of the target bed. The computed tuning thickness is about 30 meters at Pohokura-1 well and 28 meters at Pohokura-3 well. Therefore, the sandstone thicknesses at both wells are below the tuning thickness. Conventional interpretation of seismic data, therefore, cannot visualize this thin bed. Hydrocarbon accumulates in TSM thin bed at Pohokura-1, but it is not present in Pohokura-3. The seismic data were then interpreted to locate thin beds. The discontinuity of the horizons was interpreted as faults. The interpretation of TSM and BSM horizons are shown in the cross section between Pohokura-1 and -3 well (Fig. 5). Fig. 6 shows the TSM time-structural map, which indicates the anticline structure in the southeast of the study area. There are reverse faults and a normal fault in the west part of the anticline. Fig. 7 shows the amplitude map of the TSM horizon with a high anomaly within the anticline structure.

A. Instantaneous Seismic Attribute Results

Fig. 8 is the instantaneous frequency map of the TSM horizon. The high anomaly of instantaneous frequency around well locations delineate a thin bed reservoir.

The map of the seismic envelope (instantaneous amplitude) of the TSM horizon (Fig. 9) shows a high anomaly that relates to the hydrocarbon bearing zone. At Pohokura-1 well, the seismic envelope has high values, but at Pohokura-3 well the values are lower. The result corresponds to the well log data at the top Mangahewa Formation. The density-neutron crossover indicates the gas bearing zone. This crossover presents in Pohokura-1 well but does not present in Pohokura-3 well (see in Figs. 3 and 4 in third tracks).

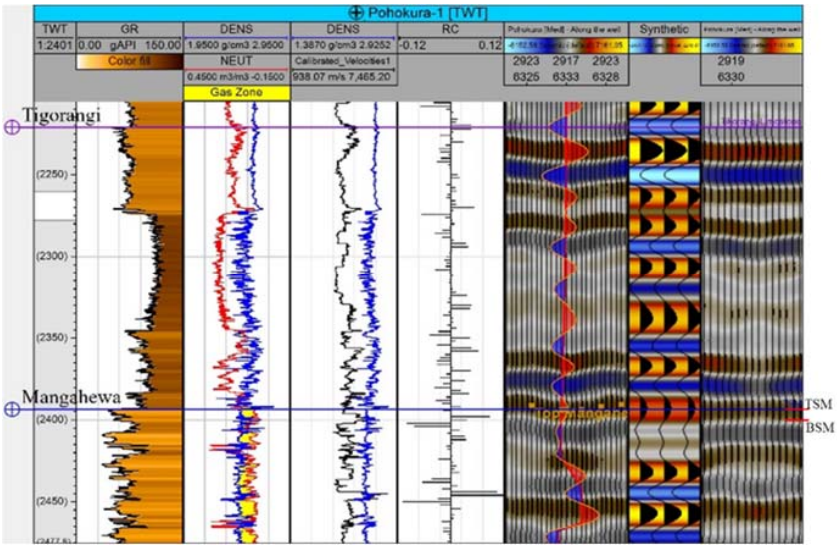

Fig. 3 Well to seismic correlation of Pohokura-1 well with 0.850 correlation over the interval 2225-2480 ms

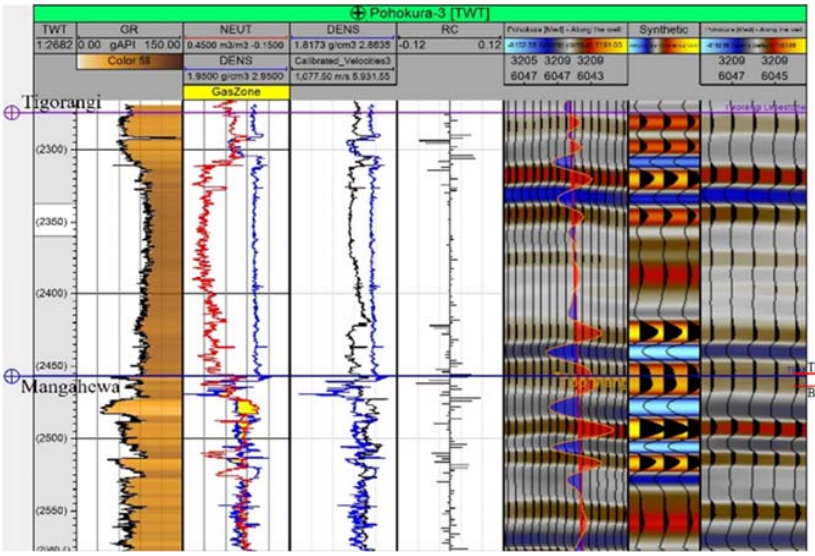

Fig. 4 Well to seismic correlation of Pohokura-3 well with 0.841 correlation over the interval 2280-2530 ms

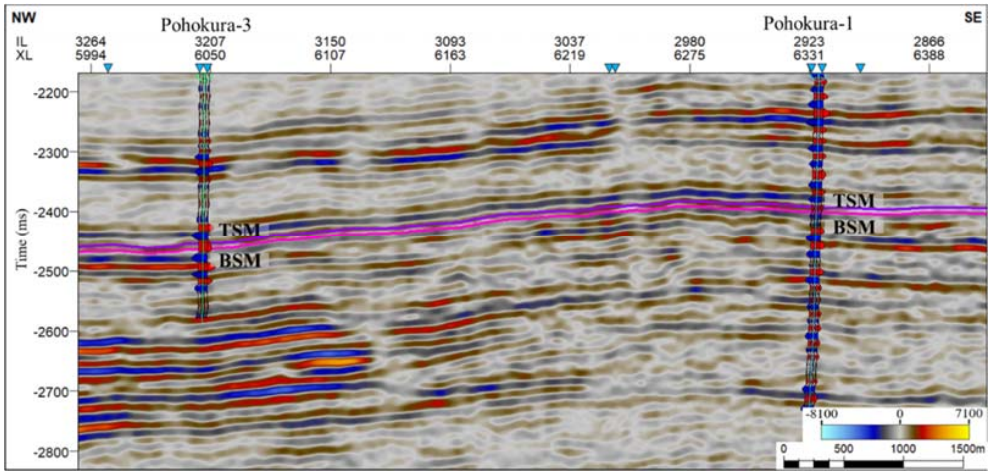

Fig. 5 Cross section between Pohokura-3 and -1 wells. Purple and pink lines are TSM and BSM horizons, respectively

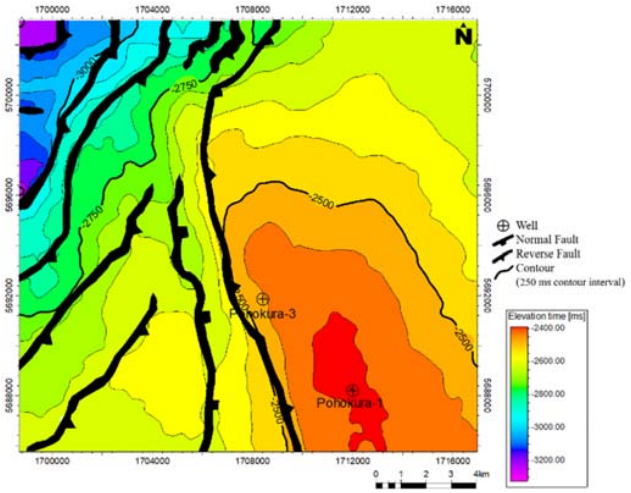

Fig. 6 TSM time-structural map

B. Spectral Decomposition Results

SWDFT spectral decomposition requires 2 parameters, the window length and the selected isofrequency. Parameter testing showed the optimal window length to be 48 ms. Then, the frequencies were selected from the spectrogram of the traces at Pohokura-1 and Pohokura-3 wells. The SWDFT spectrogram of Pohokura-1 well is shown in Fig. 10. The Pohokura 3D seismic data processing report [18] stated that a 4/8/70/80 Hz bandpass filter was applied; therefore, the tested frequencies should not be over 80 Hz. Comparing the 56-Hz, 72-Hz and 80-Hz isofrequency SWDFT maps of the TSM horizon (Fig. 11), the high anomaly of 72 Hz isofrequency SWDFT (Fig. 11 (b)) clearly delineates a thin bed between TSM and BSM horizons.

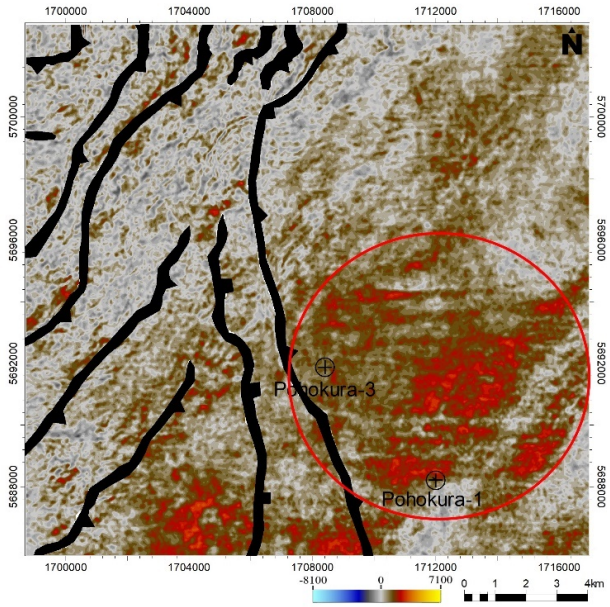

Fig. 7 Amplitude map of TSM horizon. The red circle indicates the high amplitude within the anticline structure

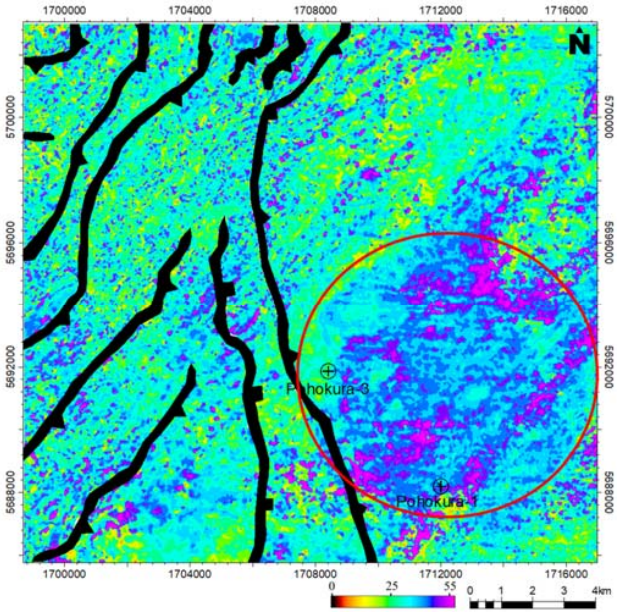

Fig. 8 Instantaneous frequency map of TSM Horizon. The red circle indicates the high anomaly instantaneous frequency which are related to thin bed reservoir

The hydrocarbon bearing zone was indicated by CWT spectral decomposition. CWT spectral decomposition requires selecting the mother wavelet. The results of each wavelet are shown in the time-frequency spectrograms (Fig. 12) at Pohokura-1 well. The suitable wavelet for these seismic data is the Mexican Hat wavelet (Fig. 12 (c)). The Mexican Hat wavelet has an ability to capture the frequency contents that better than other wavelets. There are 2 criteria for hydrocarbon indication, which are a low frequency shadow zone below the reservoir level and an abnormal seismic attenuation in higher isofrequency CWT spectral decomposition. Comparing to the seismic amplitude map of BSM horizon (Fig. 13 (a)), the 30 Hz isofrequency map (Fig. 13 (b)) clearly shows a high anomaly of low frequency shadow below the thin bed reservoir. The low frequency shadow anomaly partially disappears in the 56 Hz isofrequency CWT map (Fig. 13 (c)) and fully disappears in the 72 Hz isofrequency CWT map (Fig. 13 (d)).

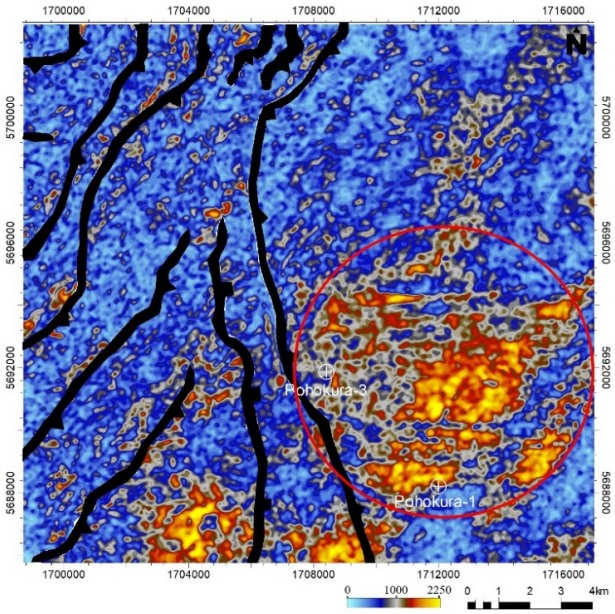

Fig. 9 Envelope map of TSM horizon. The red circle indicates the high anomaly of envelope which are related to hydrocarbon bearing zone

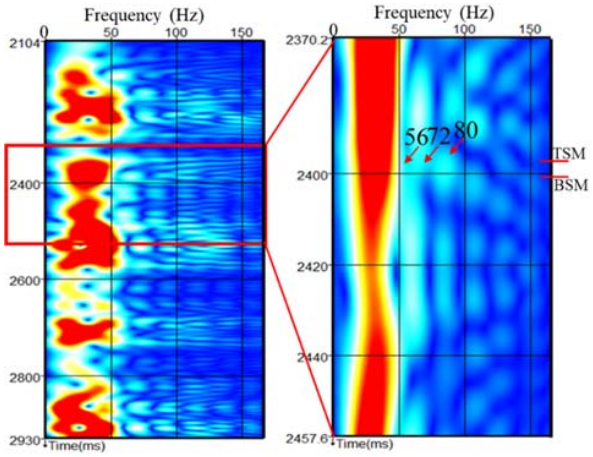

Fig. 10 Time-frequency spectrogram of Pohokura-1 well at Inline-2917 and Crossline-6332

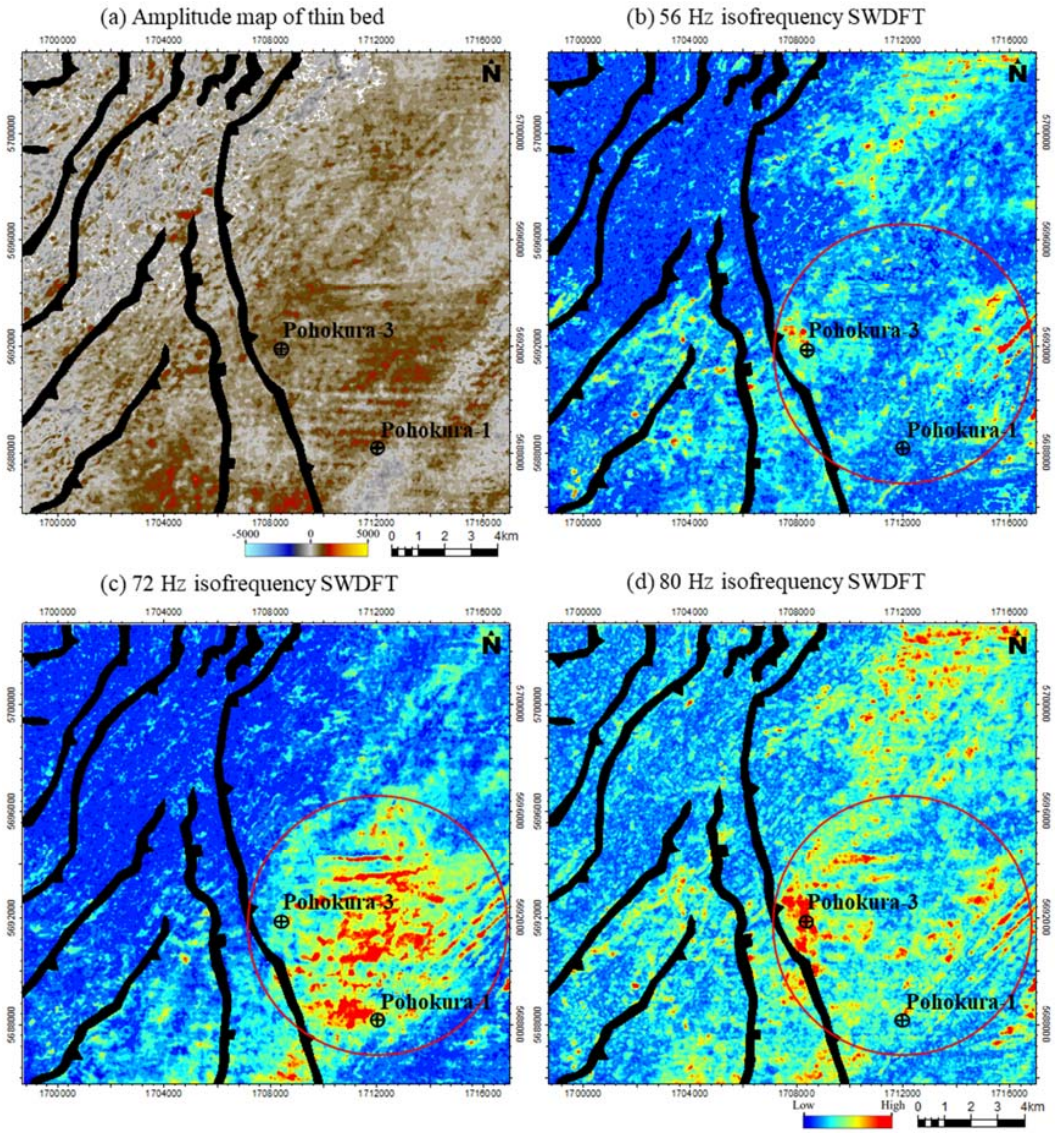

Fig. 11 SWDFT isofrequency maps for (a) 56 Hz, (b) 72 Hz, and (c) 80 Hz with 48 ms window length

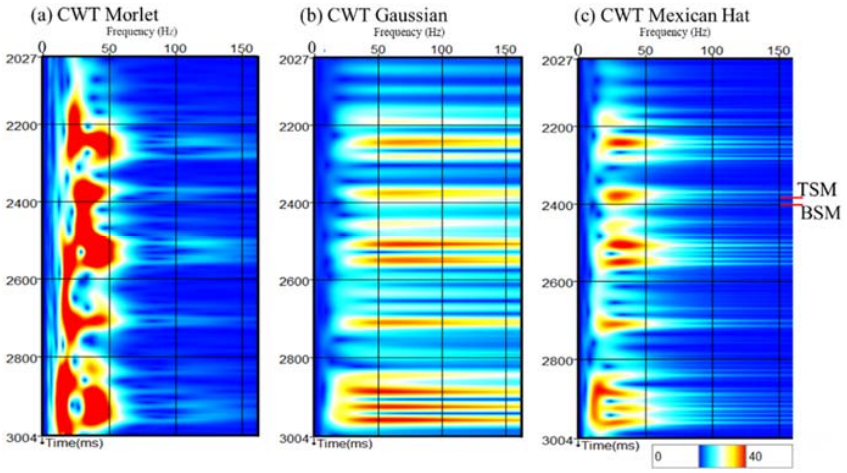

Fig. 12 CWT spectral decomposition spectrogram computed using (a) Morlet, (b) Gaussian, and (c) Mexican Hat wavelet

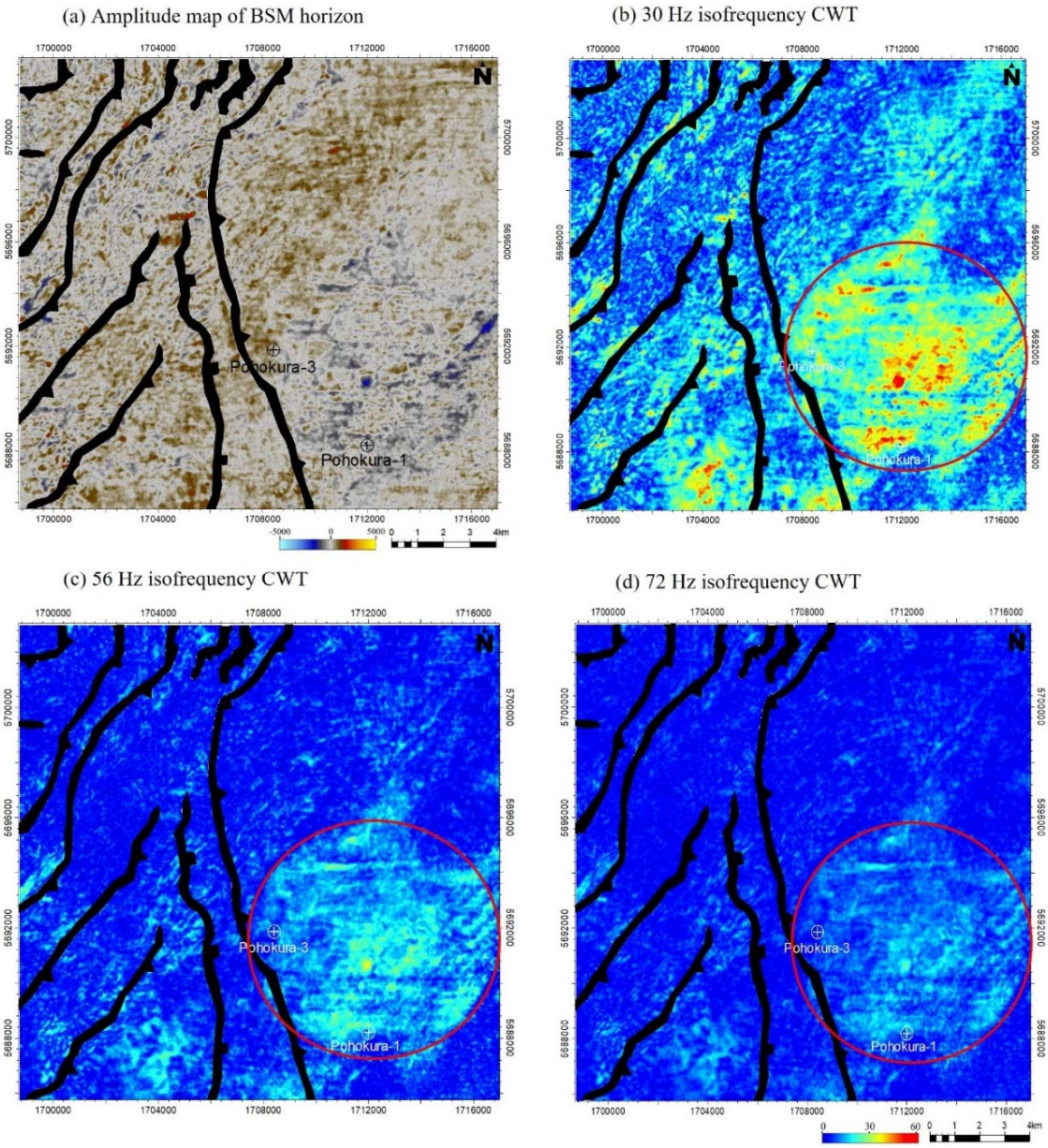

Fig. 13 CWT isofrequency maps below the reservoir using a Mexican hat wavelet: (a) amplitude map, (b) 30 Hz, (c) 56 Hz, and (d) 72 Hz. Red circle indicates the location of hydrocarbon

IV. Discussion and Conclusion

Sinha et al. [10] suggested that CWT spectral decomposition has an ability to capture the frequency contents better than SWDFT spectral decomposition. In contrast, the SWDFT spectral decomposition is more accurate in time resolution than CWT spectral decomposition due to the fixed window length. The 72-Hz isofrequency sections (Fig. 14) indicate that SWDFT spectral decomposition can clearly delineate a thin bed reservoir, but CWT spectral decomposition cannot reveal the thin bed at the target zone. In this study area, the result from SWDFT spectral decomposition is more reliable to delineate thin bed than CWT spectral decomposition.

In conclusion, SWDFT spectral decomposition can reveal the thin bed using a 72-Hz isofrequency map and section. In addition, the instantaneous frequency attribute (Fig. 8) indicates the thin beds at the same location of the 72-Hz isofrequency section by using the frequency spike. For the hydrocarbon bearing zone, the envelope highlights the location that has the potential to be the hydrocarbon accumulation zone. Additionally, the CWT spectral decomposition can reveal the low-frequency shadow below the hydrocarbon accumulation and the abnormal seismic attenuation of higher isofrequency content, which would be the indication of hydrocarbon bearing zone. Therefore, the thin bed reservoir, whose thickness is below the seismic vertical resolution, can be delineated by SWDFT spectral decomposition and instantaneous frequency

attribute, while the hydrocarbon bearing zone can be indicated by CWT spectral decomposition and envelope attribute.

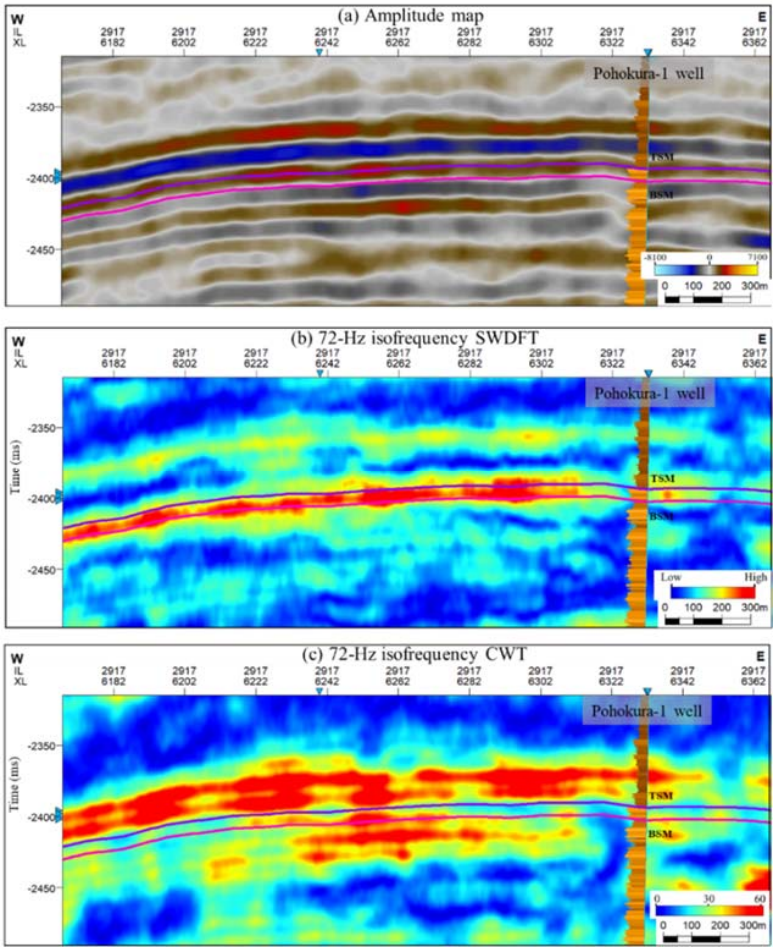

Fig. 14 Comparison of 72 Hz isofrequency from (a) amplitude, (b) SWDFT, and (c) CWT spectral decompositions sections at Inline-2917.# Pohokura-1 well shows gamma ray log which yellow color indicates relative low gamma ray values and brown color indicates relative high gamma ray values

ACKNOWLEDGMENT

The author would like to thank Schlumberger S.A. Overseas and dGB Earth Sciences for providing the software, New Zealand Petroleum & Minerals (NZP&M) for the seismic datasets, and PTT Exploration and Production Public Company Limited (PTTEP), and Faculty of Science, Chiang Mai University for the financial support, Dr. Robert Kieckhefer#for language editing and reviewing the paper1

REFERENCES

[1] Ministry of Business, Innovation and Employment, 2018, Energy in New Zealand 2018, https://www.mbie.govt.nz/assets/d7c93162b8/energy-in-nz-18.pdf, accessed 10 January 2020.
[2] New Zealand Petroleum and Minerals, 2014a, NZP&M Data, http://nzpam.govt.nz/home/Maps_and_geoscience_data/Petroleum_Exploration_Data_Pack/ArcGIS_Project/ArcMap_Project/GIS_Viewer_10-x.mxd, accessed 22 February 2020.
[3] New Zealand Petroleum and Minerals, 2014b, Petroleum Fields, http://nzpam.govt.nz/home/Maps_and_geoscience_data/Petroleum_Exploration_Data_Pack/ArcGIS_Project/ArcMap_Project/GIS_Viewer_10-x.mxd, accessed 22 February 2020.
[4] New Zealand Outline Png, 2021, https://pngio.com/images/pngb2049507.html, accessed 29 May 2021.
[5] Ministry of Business, Innovation and Employment, 2014, New Zealand Petroleum Basin part one, https://www.nzpam.govt.nz/assets/Uploads/doing-business/nz-petroleum-basins-part-one.pdf, accessed 22 February 2020.
[6] M. T., Taner, F. Koehler, and R.E. Sheriff, 1979, Complex seismic trace analysis: Geophysics, 44, no. 6, 1041-1063, doi: 10.1190/1.1440994.
[7] S., Koson, P. Chenrai, and M. Choowong, 2014, Seismic attributes and their application in seismic geomorphology: Bulletin of Earth Sciences of Thailand, 6, no. 1, 1-9.
[8] H., Zeng, 2010, Geologic significance of anomalous instantaneous frequency: Geophysics, 75, no. 3, 23-30, doi: 10.1190/1.3427638.
[9] L. A. G. R., Pereira, 2009, Seismic Attribute in Hydrocarbon Reservoirs Characterization, Ph.D. thesis, University of Aveiro.
[10] S., Sinha, P. S. Routh, P. D. Anno, and J. P. Castagna, 2005, Spectral decomposition of seismic data with continuous-wavelet transform: Geophysics, 40, no. 6, 19-25, doi: 10.1190/1.2127113.
[11] G., Partyka, J. Gridley, and J. Lopez, 1999, Interpretational applications of spectral decomposition in reservoir characterization: The Leading Edge, 18, no. 3, 353-360, doi: 10.1190/1.1438295.
[12] A., Kwietniak, 2016, Spectral decomposition of a seismic signal: thin bed

thickness estimate and analysis of attenuation zones: Ph.D. thesis, University of Science and Technology AGH.
[13] S., Mallat, 1999, A wavelet tour of signal processing, Academic Press.
[14] S., Chopra, and K. J. Marfurt, 2015, Choice of mother wavelet in CWT spectral decomposition, SEG New Orleans Annual Meeting 2015, SEG, Expanded Abstract, 2957-2961, doi: 10.1190/segam2015-5852193.1.
[15] A. P., Ngeri, E. D. Uko, and I. Tamunobereton-ari, 2018, The Choice of Mother Wavelet in the Application of Continuous Wavelet Transform Method of Spectral Decomposition in Field 'A' in Central Niger Delta: Asian Journal of Applied Science and Technology (AJAST), 2, no. 4, 303-314.
[16] A., Haris, I. N. Suabdi, Erwinsyah, Adriansyah, A. Nurhasan, A. Khair, and I. A. Kainama, 2008, Low frequency shadow zone analysis based on CWT spectral decomposition: case study of South Sumatra Basin: 32nd Annual Convention Proceedings, IPA, Proceedings, G-070, doi: 10.29118/ipa.797.08.g.070.
[17] M. B., Widess, 1973, How thin is a thin bed: Geophysics, 30, no. 6, 1176-1180, doi: 10.1190/1.1440403.
[18] Ministry of Economic Development New Zealand, 2006, Seismic Data Processing Report. Pohokura 3D Project Reprocessing, Unpublished Petroleum Report.